AIAA JOURNAL
Vol. 43, No. 3, March 2005

Postbuckling Behavior of Triangular Plates

M. Azhari,* A. R. Shahidi,† and M. M. Saadatpour*
Isfahan University of Technology, Isfahan, Iran
and
M. A. Bradford‡
University of New South Wales, Sydney, New South Wales 2052, Australia

A numerical method is developed for the elastic postbuckling analysis of triangular plates. The procedure uses the method of virtual work in conjunction with area coordinates. The method is programmed, and several numerical examples are presented to illustrate the efficacy and scope of the procedure. Bifurcative local buckling results obtained for triangular plates are compared with known solutions reported in the literature. The postbuckling behavior of triangular plates is then studied for different geometrical configurations, and the stress distribution and postbuckling equilibrium paths are illustrated for several triangular plates with a range of geometries.

Nomenclature

A	=	area of triangle
a	=	height of plate
$[B_f]$, $[B_m]$	=	flexural and membrane strain matrices
b	=	width of plate
C	=	computational domain
$[D_f]$, $[D_m]$	=	flexural and membrane property matrices
E	=	Young's modulus
$\{F\}$	=	vector of forces
$[J]$	=	tangent stiffness matrix
$[J_1]$, $[J_2]$	=	first- and second-order Jacobian matrices
$[K_{\mathrm{NL}}]$	=	nonlinear stiffness matrix
L_1, L_2, L_3	=	area coordinates
M_x, M_y, M_{xy}	=	flexural bending and torsional moments
$\bar{N}_{\mathrm{cr}}$	=	critical eigenvalue
$N_i^{(u)}$, $N_i^{(v)}$, $N_i^{(w)}$	=	shape functions for the u, v, and w displacements
N_u, N_v, N_w	=	number of shape functions for u, v, and w displacements
N_x, N_y, N_{xy}	=	membrane normal and shear forces
n	=	P_x/P_y
P_x, P_y	=	loads in x and y directions, respectively
$\mathcal{P}$	=	physical domain
p, q, r	=	polynomial integral powers
t	=	thickness of plate
u, v	=	membrane displacements in x and y directions
u_H, v_H	=	membrane displacements caused by Hookean shortening
w	=	flexural displacement
w_0	=	flexural displacement at $(x, y) = (a/2, b/2)$
x, y	=	Cartesian coordinates
x_i, y_i	=	Cartesian coordinates of corner i
α_i, β_i, γ_i	=	factors defined in Eq. (4)
$\{\Delta\}$	=	vector of deformations
ε_{x0}, ε_{y0}	=	compressive strains in x and y directions
$\{\varepsilon_f\}$, $\{\varepsilon_m\}$	=	linear flexural and geometric nonlinear strain vectors
λ	=	local buckling coefficient
ν	=	Poisson's ratio
$\{\sigma_f\}$, $\{\sigma_m\}$	=	flexural and membrane stress vectors

Received 31 December 2001; accepted for publication 14 July 2004.

*Professor, Department of Civil Engineering.
†Graduate Student, Department of Civil Engineering.
‡Scientia Professor, School of Civil and Environmental Engineering.

I. Introduction

THIN triangular plates are used commonly in aeronautical and aerospace construction, where they are often required to carry substantial compressive in-plane stress. Under in-plane compressive loading, the buckling and postbuckling behavior of triangular plates can be of great significance and must be quantified. Although a review of the existing open literature indicates that many studies have been undertaken for the buckling and vibration of triangular plates, investigations reporting the postbuckling response of triangular plates are very scant. This paper is thus concerned with the elastic postbuckling behavior of triangular plates.

Substantial weight savings can be achieved by utilizing the postbuckling response of plate structures. In the postbuckled domain, the buckled configuration of a triangular plate is still stable owing to benign membrane actions that develop after it buckles locally. Because of this, triangular plates have a significant reserve of strength prior to collapse that is usually instigated by plasticity, and this strength reserve must be utilized in efficient weight-minimization aerospace and advanced structural engineering applications.

Studies of the buckling of triangular plates date back some seven decades. A buckling analysis of simply supported equilateral triangular plates was first presented by Woinowsky-Krieger[1] in 1933 and then by Taylor[2] in 1957. Klitchieff[3] studied the stability of simply supported right-angled isosceles triangular plates subjected to in-plane shear stresses. Klitchief's solution was then improved on in 1955 by Wittrick,[4] who included combined in-plane normal loads and different boundary conditions, whereas Pan[5] obtained the buckling solution for a ply-supported triangular plate under compression. The stability of simply supported isosceles triangular orthotropic plates, subjected to combined in-plane loading, was studied much later by Valisetty and Reddy.[6]

More recently, Liew and Wang[7] employed their so-called pb-2 Rayleigh–Ritz method to study the elastic buckling of rectangular plates with internal curved supports. They also studied the elastic buckling of triangular plates with internal line supports under uniform compression.[8] Their solution includes different boundary conditions, and they presented buckling factors that were valuable for a designer seeking the buckling loads of right-angled and isosceles triangular plates of various height-to-base ratios. Jaunky et al.[9] used the Rayleigh–Ritz method combined with a variational formulation to obtain buckling factors of general triangular anisotropic plates with different boundary conditions subjected to combined in-plane stresses. Their analytical formulation provided accurate buckling load results for isotropic and anisotropic triangular plates that are useful in the design of grid-stiffened structures.[9]

The postbuckling analysis of rectangular plates has been studied to a much larger extent than that of arbitrary quadrilateral plates. Azhari and Bradford[10] used a bubble finite strip method employing orthogonal Legendre polynomials to study the postlocal buckling of plate assemblies, whereas the postbuckling response of biaxially compressed plates on an elastic foundation was investigated by Jayachandran and Vaidyanathan[11] using the Lagrangean finite-element procedure. The mixed Galerkin perturbation technique was employed by Shen and Lin[12] to determine the postbuckling equilibrium paths of antisymmetrical angle-ply and symmetrically cross-ply laminate plates. Hoon and Khong[13] used a combination of the Rayleigh–Ritz and finite-strip methods to investigate the postbuckling behavior of uniformly compressed rectangular plates.

Shen[14] analyzed the thermomechanical postbuckling response of imperfect, antisymmetrical angle-ply and symmetric cross-ply laminated plates subjected to the combined loading of a uniform temperature rise and of axial compression. The thermal postbuckling analysis of imperfect, shear-deformable symmetric cross-ply laminated plates on an elastic foundation under a nonuniform temperature field was investigated by Shen.[15] Recently, Shen[16] used a mixed Galerkin perturbation technique to determine the postbuckling equilibrium paths of preloaded shear-deformable laminated plates. To the authors' knowledge, no work on the postbuckling of triangular plates has been reported openly. The present paper describes a numerical procedure for studying the postbuckling behavior of triangular plates, including appropriate Hookean shortening. The procedure is based on the method of work and uses natural area coordinates.

II. Theory

A. General

Consider an elastic, isotropic, flat triangular plate of constant thickness t and height-to-width ratio b/a, as shown in Fig. 1. The plate is subjected to an in-plane uniform compressive stress field. The basic steps in the postbuckling analysis, as developed in this section, involve the following:

1) A transformation of the physical domain $\mathcal{P}(x, y)$ into a computational domain C defined by an area coordinate system (L_1, L_2, L_3).

2) A definition of the Hookean shortening and displacement functions in order to describe the membrane and flexural behavior of a triangular plate. These functions are selected a priori to satisfy the in-plane and out-of-plane boundary conditions.

3) Selection of an appropriate elastic plate theory to describe the membrane and flexural behavior of a triangular plate.

4) Invoking the principle of stationary potential energy to determine the nonlinear governing equation that describes the postbuckling equilibrium paths.

5) Solution of the nonlinear equations by deploying the Newton–Raphson procedure for a triangular plate and subjected to increasing compressive strain.

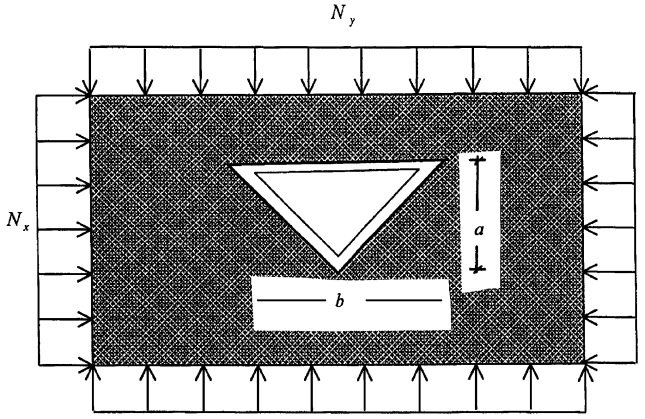

Fig. 1 Postbuckling of triangular plate subjected to in-plane uniform pressure along its edges.

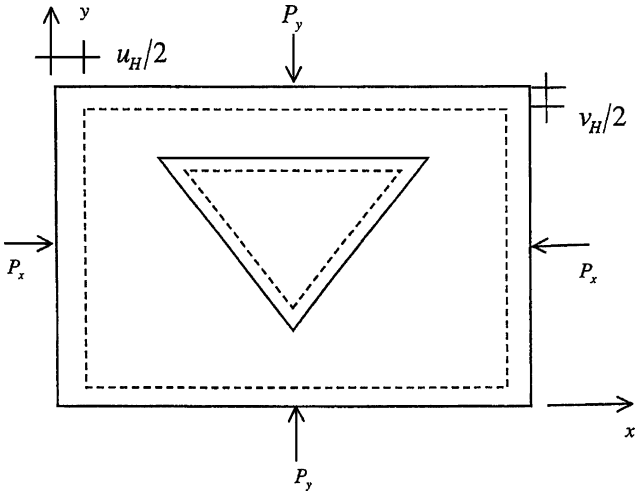

Fig. 2 Hookean displacements of triangular plate.

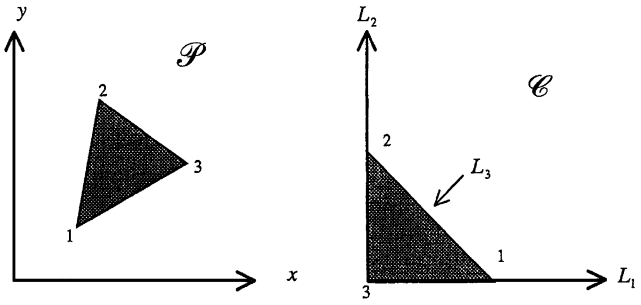

Fig. 3 Physical and computational domains.

B. Domain Transformation

The formulation of the postbuckling analysis for general triangular plates (Fig. 2) subjected to in-plane loads is performed by transforming the physical domain $\mathcal{P}(x, y)$ into a computational domain C defined by an area coordinate system L_1, L_2, L_3 (Fig. 3) using the following mapping:

$$x(L_1, L_2) = L_1 x_1 + L_2 x_2 + (1 - L_1 - L_2) x_3 \tag{1}$$

$$y(L_1, L_2) = L_1 y_1 + L_2 y_2 + (1 - L_1 - L_2) y_3 \tag{2}$$

$$L_i = (1/2A)(\alpha_i + \beta_i x + \gamma_i y) \tag{3}$$

in which

$$2A = \begin{vmatrix} x_1 & x_2 & x_3 \\ y_1 & y_2 & y_3 \\ 1 & 1 & 1 \end{vmatrix}, \qquad \alpha_i = x_j y_k - y_j x_k$$

$$\beta_i = y_j - y_k, \qquad \gamma_i = x_k - x_j \tag{4}$$

where $L_i\ (i = 1, 2, 3) \in C$ are the area coordinates and $x_i\ (i = 1, 2, 3) \in \mathcal{P}$ and $y_i\ (i = 1, 2, 3) \in \mathcal{P}$ are the physical coordinates of the ith corner of the plate. It should be noted that the third area coordinate is expressed in terms of the others by $L_3 = (1 - L_1 - L_2)$.

A transformation of the physical domain to the computational domain is necessary so that the boundary conditions cam be imposed easily. The first- and second-order Jacobian matrices of the transformation, $[J_1]$ and $[J_2]$, respectively, are defined as

$$[J_1] = \begin{bmatrix} \dfrac{\partial x}{\partial L_1} & \dfrac{\partial y}{\partial L_1} \\ \dfrac{\partial x}{\partial L_2} & \dfrac{\partial y}{\partial L_2} \end{bmatrix} = \begin{bmatrix} \gamma_2 & \beta_2 \\ \gamma_1 & \beta_1 \end{bmatrix} \tag{5}$$

$$[J_2] = \begin{bmatrix} \gamma_2^2 & \beta_2^2 & 2\beta_2\gamma_2 \\ \gamma_1^2 & \beta_1^2 & 2\beta_1\gamma_1 \\ \gamma_1\gamma_2 & \beta_1\beta_2 & \beta_1\gamma_2 + \beta_2\gamma_1 \end{bmatrix} \tag{6}$$

By applying the chain rule of differentiation, it can be shown simply that the first and second derivatives are related by

$$\begin{Bmatrix} \dfrac{\partial}{\partial x} \\ \dfrac{\partial}{\partial y} \end{Bmatrix} = [J_1]^{-1} \begin{Bmatrix} \dfrac{\partial}{\partial L_1} \\ \dfrac{\partial}{\partial L_2} \end{Bmatrix}, \qquad \begin{Bmatrix} \dfrac{\partial^2}{\partial x^2} \\ \dfrac{\partial^2}{\partial y^2} \\ \dfrac{\partial^2}{\partial x \partial y} \end{Bmatrix} = [J_2]^{-1} \begin{Bmatrix} \dfrac{\partial^2}{\partial L_1^2} \\ \dfrac{\partial^2}{\partial L_2^2} \\ \dfrac{\partial^2}{\partial L_1 \partial L_2} \end{Bmatrix} \tag{7}$$

C. Displacement Field

The triangular plate shown in Fig. 2 is assumed to be compressed in its plane by frictionless platens located at its ends, such as those of a heavy testing machine. The in-plane compressive strains are assumed to be ε_{x0} and ε_{y0} in the x and y directions, respectively. The resulting membrane-displacement field in the rectangular plate is defined by the displacements u and v in the x and y directions respectively. These membrane displacements consist of two components: those arising from Hookean shortening (u_H and v_H in Fig. 2) and those arising from the geometric nonlinear components resulting from plate flexure. The main advantage of the inclusion of Hookean shortening is that, in the postbuckling analysis, the total potential energy is formulated as a function of the compressive strains ε_{x0} and ε_{y0} rather than the stresses, because the stress distribution changes from an initial uniform distribution in the postbuckling range.[10,17]

In Fig. 2, the dashed line represents the deformed shape of the triangular plate. If the magnitude of the ratio of the loads in the x and y directions is considered to be $P_x/P_y = n$, so that $u_H/v_H = n$ and $\varepsilon_{x0}/\varepsilon_{y0} = n$, then $\varepsilon_{x0} = \varepsilon_0$ and $\varepsilon_{y0} = \varepsilon_0/n$ are the Hookean strains.

The in-plane displacements u and v corresponding to the sum of the Hookean deformations, and the geometric nonlinear components of the membrane displacements that occur as a result of the flexural displacements of the triangular plates are given by

$$u = \sum_{i=1}^{N_u} N_i^{(u)} \hat{u}_i + u_H \tag{8}$$

$$v = \sum_{i=1}^{N_v} N_i^{(v)} \hat{v}_i + v_H \tag{9}$$

whereas the flexural displacement field normal to the plate is given by

$$w = \sum_{i=1}^{N_w} N_i^{(w)} \hat{w}_i \tag{10}$$

where $N_i^{(u)}$ $(i = 1, \ldots, N_u)$, $N_i^{(v)}$ $(i = 1, \ldots, N_v)$, and $N_i^{(w)}$ $(i = 1, \ldots, N_w)$ are the ith shape functions in terms of the area coordinates L_1 and L_2 and are approximated independently by polynomial functions of the type $(L_1)^p \times (L_2)^q \times (1 - L_1 - L_2)^r$, where p, q, and r are integers. In Eqs. (8–10), $\hat{u}_i$ $(i = 1, \ldots, N_u)$, $\hat{v}_i$ $(i = 1, \ldots, N_v)$, and $\hat{w}_i$ $(i = 1, \ldots, N_w)$ are the unknown generalized deformations to be determined.

D. Strains and Stresses

The generalized flexural strain vector $\{\varepsilon_f\}$ is given by

$$\{\varepsilon_f\} = \langle -w_{,xx}\,;\, -w_{,yy}\,;\, -2w_{,xy} \rangle^T \tag{11}$$

whereas from familiar nonlinear plate theory, the membrane strain vector including only those nonlinear terms associated with plate flexure is represented by

$$\{\varepsilon_m\} = \left\langle \left(u_x + \tfrac{1}{2}w^2{}_{,x}\right);\, \left(v_y + \tfrac{1}{2}w^2{}_{,y}\right);\, (u_{,y} + v_{,x} + w_{,x}\, w_{,y}) \right\rangle^T \tag{12}$$

where commas denote partial differentiation.

The displacement fields are substituted into Eqs. (11) and (12), and membrane and flexural strains are expressed in terms of the generalized coordinates by

$$\{\varepsilon_m\} = [T_u]\{\hat{u}\} + [T_v]\{\hat{v}\} + \tfrac{1}{2}[T_w]\{\hat{w}\} + \{\varepsilon_H\} \tag{13}$$

$$\{\varepsilon_f\} = [B_f]\{\hat{w}\} \tag{14}$$

where $\{\varepsilon_H\}$ is the Hookean strain vector and $[T_u]$, $[T_v]$, $[T_w]$, and $[B_f]$ are given in Appendix A.

The generalized stress vectors containing the bending moments and torsional moments per unit length of the plate $\{\sigma_f\}$ and the membrane normal and shear forces per unit thickness $\{\sigma_m\}$ are

$$\{\sigma_f\} = \langle M_x;\, M_y;\, M_{xy} \rangle^T \tag{15}$$

$$\{\sigma_m\} = \langle N_x;\, N_y;\, N_{xy} \rangle^T \tag{16}$$

and these vectors are used in the following derivation.

E. Elastic Plate Theory

The study here is restricted for simplicity to elastic isotropic plates, although it may easily be extended to orthotropic plates. The plate property matrices that define the membrane and flexural constitutive relationships are, respectively,

$$\{\sigma_f\} = [D_f]\{\varepsilon_f\} \tag{17}$$

$$\{\sigma_m\} = [D_m]\{\varepsilon_m\} \tag{18}$$

where

$$[D_m] = \begin{bmatrix} 1 & \nu & 0 \\ \nu & 1 & 0 \\ 0 & 0 & (1-\nu)/2 \end{bmatrix}, \qquad [D_f] = \frac{t^3}{12}[D_m] \tag{19}$$

in which E is Young's modulus of elasticity, ν is Poisson's ratio, and t is the thickness of the plate.

F. Principle of Virtual Work and Equilibrium Equations

Because the postbuckling equilibrium path is controlled by the Hookean strains, and because the edges are held straight, the principle of virtual work can be stated as

$$\int_{\mathcal{P}} \{\delta\varepsilon_m\}^T \{\sigma_m\}\, \mathrm{d}\mathcal{P} + \int_{\mathcal{P}} \{\delta\varepsilon_f\}^T \{\sigma_f\}\, \mathrm{d}\mathcal{P} \tag{20}$$

where $\mathcal{P}$ is the physical domain of the plate. Using Eqs. (13–19), the preceding equation may be written in terms of the generalized coordinates as

$$\int_{\mathcal{P}} \left(\{\delta\hat{u}\}^T[T_u]^T + \{\delta\hat{v}\}^T[T_v]^T + \{\delta\hat{w}\}^T[T_w]^T\right)[D_m] \times \left([T_u]\{\hat{u}\} + [T_v]\{\hat{v}\} + \tfrac{1}{2}[T_w]\{\hat{w}\} + \{\varepsilon_H\}\right) \mathrm{d}\mathcal{P} + \int_{\mathcal{P}} \{\delta\hat{w}\}^T[B_f]^T[D_f][B_f]\{\hat{w}\}\, \mathrm{d}\mathcal{P} = 0 \tag{21}$$

where Gaussian quadrature is used to integrate the polynomial functions contained within these stiffness relationships. After some mathematical manipulation, the nonlinear equilibrium equations may be written as

$$\begin{pmatrix} [T_{uu}] & [T_{uv}] & [T_{uw}] \\ [T_{vu}] & [T_{vv}] & [T_{vw}] \\ [T_{wu}] & [T_{wv}] & [T_{ww}] \end{pmatrix} \begin{Bmatrix} \{\hat{u}\} \\ \{\hat{v}\} \\ \{\hat{w}\} \end{Bmatrix} + \begin{Bmatrix} \{F_u\} \\ \{F_v\} \\ \{F_w\} \end{Bmatrix} = \{0\} \tag{22}$$

where the matrices $[T_{uu}], \ldots, [T_{ww}]$ and $\{F_u\}, \ldots, \{F_w\}$ are given in Appendix B.

G. Solution of the Nonlinear Equilibrium Equation

Equation (22) may be written in the familiar stiffness form as

$$[K_{\mathrm{NL}}]\{\Delta\} + \{F\} = \{0\} \tag{23}$$

For implementation of the nonlinear analysis, the Newton–Raphson method has been used. The nonlinear analysis must proceed from an estimate of $\{\Delta\}$ and improve upon the estimate in succeeding iterations. The improved displacement vector $\{\Delta\}^{r+1}$ is given by

$$\{\Delta\}^{r+1} = \{\Delta\}^{r} - [J]^{-T}\left([K_{\mathrm{NL}}]\{\Delta\}^{r} + \{F\}^{r}\right) \tag{24}$$

where the superscript r denotes the rth iteration cycle and $[J]$ is the tangent stiffness matrix. The ith column of $[J]$, is shown as $(J)_i$ and is given by

$$(J)_i = (K_{\mathrm{NL}})_i \qquad \text{if} \quad i \le N_u + N_v \tag{25}$$

$$(J)_i = [K_{\mathrm{NL}}]_{,j}\{\Delta\} + (K_{\mathrm{NL}})_j + \{F\}_{,j}$$

$$\text{if} \quad i > N_u + N_v, \qquad j = i - N_u - N_v \tag{26}$$

where $(K_{\mathrm{NL}})_i$ is the ith column of the nonlinear matrix $[K_{\mathrm{NL}}]$ and the components of $[K_{\mathrm{NL}}]_{,j}$ and $\{F\}_{,j}$ are given in Appendix C.

The Jacobian $[J]$ should be updated in every iteration cycle and the following convergence criterion was used to terminate the iterations at every step:

$$\frac{\|\{\Delta\}^{r+1} - \{\Delta\}^{r}\|}{\|\{\Delta\}^{r}\|} \le 0.1\% \tag{27}$$

III. Numerical Studies

A. General

The nonlinear virtual work method described in the preceding section was programmed, and some numerical results are presented here for the buckling and postbuckling of triangular plates with different geometries and in-plane loading conditions.

To demonstrate the accuracy and convergence of the method, a geometrically perfect simply supported right-angled triangular plate whose longitudinal edges are held straight was analyzed. The shape functions in Eqs. (8–10) were chosen to satisfy the condition of simple supports, in that both the functions themselves and their second derivatives vanished at the supports. Equation (23) can be recast simply as a linear eigenproblem appropriate to local buckling by allowing the nonlinear terms to vanish. This problem has been investigated by Jaunky et al.[9] and by Wang and Liew.[8]

The results for triangular plates have been nondimensionalized and expressed in terms of a local buckling coefficient λ by

$$\lambda = \bar{N}_{\mathrm{cr}} a^2/\pi^2 D \tag{28}$$

where a is the dimension of the triangular plate in the x direction, $\bar{N}_{\mathrm{cr}}$ is the critical eigenvalue, and D is the plate rigidity.

Table 1 presents the local buckling coefficients λ for right-angled simply supported plates for various width-to-height ratios $a/b = 1$, 2/3, 1/2, 2/5, 1/3, 2/7, and 1/4. The results from this method correlate very well with those presented by Wang and Liew.[8]

B. Postbuckling Behavior of Triangular Plates

1. Convergence Study

Table 2 demonstrates the convergence characteristics for the nondimensional displacements w_0/t of a right-angled isosceles simply supported triangular plate ($x = a/2$, $y = b/2$) subjected to compression. The table shows that for different values of $\varepsilon/\varepsilon_{\mathrm{cr}}$ ($\varepsilon_{\mathrm{cr}}$ being the local buckling strain), the nondimensional displacements in the postbuckling region converge very well within eight iterations. Moreover, based on these convergence studies it was established that 16 sets of polynomial functions ($N_u = N_v = N_w = 16$), whose indices p, q, r are such that the conditions of a simple support are satisfied, are sufficient to obtain very accurate solutions.

Table 1 Buckling factors $\lambda = \bar{N}_{\mathrm{cr}} a^2/\pi^2 D$ for a simply supported right-angled triangular plate

	a/b						
Method	1	2/3	1/2	2/5	1/3	2/7	1/4
Present	4.988	3.425	2.820	2.525	2.276	2.061	1.934
Wang and Liew[8]	5.000	3.473	2.812	2.517	2.213	2.051	1.932

Table 2 Convergence of nondimensional displacements w_0/t for a right-angled isosceles simply supported triangular plate subjected to compression

	Number of iterations							
$\varepsilon/\varepsilon_{\mathrm{cr}}$	1	2	3	4	5	6	7	8
1.5	0.8059	0.5843	0.4591	0.4048	0.3930	0.3926	0.3924	0.3924
2.0	0.8405	0.6586	0.5789	0.5610	0.5609	0.5608	0.5600	0.5600
2.5	0.8786	0.7383	0.6953	0.6910	0.6909	0.6909	0.6909	0.6909
3.0	0.9210	0.8222	0.8035	0.8030	0.8029	0.8028	0.8028	0.8028
3.5	0.9687	0.9086	0.9029	0.9028	0.9027	0.9026	0.9026	0.9026
4.0	1.0236	0.9953	0.9950	0.9946	0.9944	0.9942	0.9942	0.9942

Table 3 Postbuckling behavior of right-angled triangular plate subjected to biaxial compression

a/b	λ	$\varepsilon/\varepsilon_{\mathrm{cr}} = 1.2$	$\varepsilon/\varepsilon_{\mathrm{cr}} = 1.5$	$\varepsilon/\varepsilon_{\mathrm{cr}} = 2.0$
0.25	1.934	$P/P_{\mathrm{cr}} = 1.092$ $w_0/t = 0.039$	$P/P_{\mathrm{cr}} = 1.480$ $w_0/t = 0.109$	$P/P_{\mathrm{cr}} = 1.908$ $w_0/t = 0.298$
0.50	2.820	$P/P_{\mathrm{cr}} = 1.149$ $w_0/t = 0.302$	$P/P_{\mathrm{cr}} = 1.368$ $w_0/t = 0.484$	$P/P_{\mathrm{cr}} = 1.725$ $w_0/t = 0.690$
1.0	4.988	$P/P_{\mathrm{cr}} = 1.157$ $w_0/t = 0.247$	$P/P_{\mathrm{cr}} = 1.393$ $w_0/t = 0.393$	$P/P_{\mathrm{cr}} = 1.764$ $w_0/t = 0.501$

Table 4 Postbuckling behavior of right-angled triangular plate subjected to uniaxial compression

a/b	λ	$\varepsilon/\varepsilon_{\mathrm{cr}} = 1.2$	$\varepsilon/\varepsilon_{\mathrm{cr}} = 1.5$	$\varepsilon/\varepsilon_{\mathrm{cr}} = 2.0$
0.25	2.318	$P/P_{\mathrm{cr}} = 1.129$ $w_0/t = 0.322$	$P/P_{\mathrm{cr}} = 1.316$ $w_0/t = 0.503$	$P/P_{\mathrm{cr}} = 1.618$ $w_0/t = 0.695$
0.50	3.797	$P/P_{\mathrm{cr}} = 1.173$ $w_0/t = 0.277$	$P/P_{\mathrm{cr}} = 1.434$ $w_0/t = 0.438$	$P/P_{\mathrm{cr}} = 1.878$ $w_0/t = 0.616$
1.0	9.163	$P/P_{\mathrm{cr}} = 1.150$ $w_0/t = 0.189$	$P/P_{\mathrm{cr}} = 1.351$ $w_0/t = 0.278$	$P/P_{\mathrm{cr}} = 1.598$ $w_0/t = 0.334$

Table 5 Postbuckling behavior of isosceles triangular plate subjected to biaxial compression

a/b	λ	$\varepsilon/\varepsilon_{\mathrm{cr}} = 1.1$	$\varepsilon/\varepsilon_{\mathrm{cr}} = 1.2$	$\varepsilon/\varepsilon_{\mathrm{cr}} = 1.5$	$\varepsilon/\varepsilon_{\mathrm{cr}} = 2.0$
0.50	2.166	$P/P_{\mathrm{cr}} = 1.052$ $w_0/t = 0.227$	$P/P_{\mathrm{cr}} = 1.105$ $w_0/t = 0.321$	$P/P_{\mathrm{cr}} = 1.262$ $w_0/t = 0.506$	$P/P_{\mathrm{cr}} = 1.526$ $w_0/t = 0.714$
1.00	4.390	$P/P_{\mathrm{cr}} = 1.080$ $w_0/t = 0.193$	$P/P_{\mathrm{cr}} = 1.160$ $w_0/t = 0.273$	$P/P_{\mathrm{cr}} = 1.397$ $w_0/t = 0.431$	$P/P_{\mathrm{cr}} = 1.789$ $w_0/t = 0.610$
1.50	7.280	$P/P_{\mathrm{cr}} = 1.061$ $w_0/t = 0.145$	$P/P_{\mathrm{cr}} = 1.121$ $w_0/t = 0.205$	$P/P_{\mathrm{cr}} = 1.294$ $w_0/t = 0.323$	$P/P_{\mathrm{cr}} = 1.565$ $w_0/t = 0.455$

2. Evaluation of Deflections and Loads

The nonlinear virtual work method has been used to study the postbuckling behavior of simply supported triangular plates with various load conditions and geometries. In this section, four examples of its application are presented. The first deals with the calculation of the load carried and the deflection in a right-angled triangular plate whose perpendicular edges are subjected to uniform and equal compression, whereas the second example is a postbuckling study of a right-angled triangular plate under axial compression. Table 3 shows the nondimensional load P/P_{cr} (P_{cr} being the local buckling load) carried in the plate and the dimensionless lateral displacement w_0/t at $x = a/2$ and $y = b/2$ of a simply supported right-angled triangular plate under biaxial loading with different width-to-height ratios a/b in terms of various selected compressive strains $\varepsilon/\varepsilon_{\mathrm{cr}}$. The results of a postbuckling analysis of a simply supported right-angled triangular plate under uniaxial loads are given in Table 4, whereas the postbuckling characteristics of isosceles triangular plates under biaxial and uniaxial compressive loads are given in Tables 5 and 6, respectively.

Table 6 Postbuckling behavior of isosceles triangular plate subjected to uniaxial compression

a/b	λ	$\varepsilon/\varepsilon_{cr}=1.1$	$\varepsilon/\varepsilon_{cr}=1.2$	$\varepsilon/\varepsilon_{cr}=1.5$	$\varepsilon/\varepsilon_{cr}=2.0$
0.25	1.764	$P/P_{cr}=1.054$	$P/P_{cr}=1.109$	$P/P_{cr}=1.275$	$P/P_{cr}=1.559$
		$w_0/t=0.205$	$w_0/t=0.289$	$w_0/t=0.456$	$w_0/t=0.640$
0.50	3.588	$P/P_{cr}=1.082$	$P/P_{cr}=1.165$	$P/P_{cr}=1.427$	$P/P_{cr}=1.900$
		$w_0/t=0.217$	$w_0/t=0.305$	$w_0/t=0.472$	$w_0/t=0.644$
1.00	9.152	$P/P_{cr}=1.080$	$P/P_{cr}=1.157$	$P/P_{cr}=1.361$	$P/P_{cr}=1.575$
		$w_0/t=0.141$	$w_0/t=0.193$	$w_0/t=0.270$	$w_0/t=0.285$
1.50	17.444	$P/P_{cr}=0.968$	$P/P_{cr}=0.998$	$P/P_{cr}=1.102$	$P/P_{cr}=1.328$
		$w_0/t=0.055$	$w_0/t=0.062$	$w_0/t=0.083$	$w_0/t=0.098$

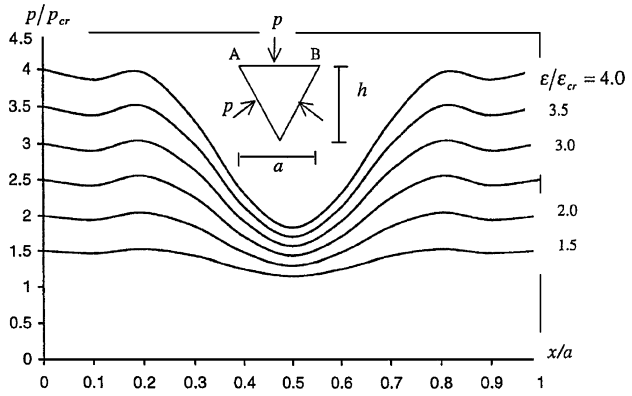

Fig. 4 Membrane stress distribution along AB for $a/h=1.0$.

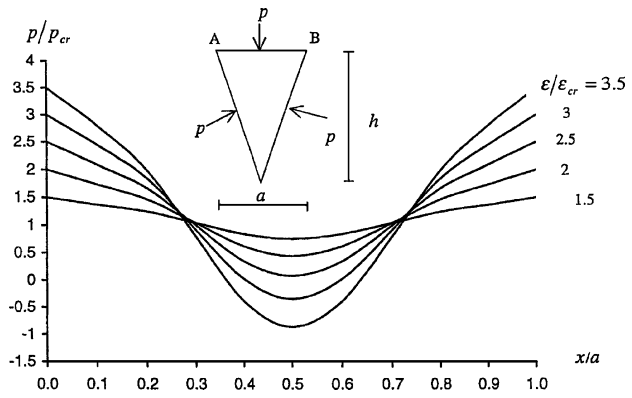

Fig. 5 Membrane stress distribution along AB for $a/h=2.0$.

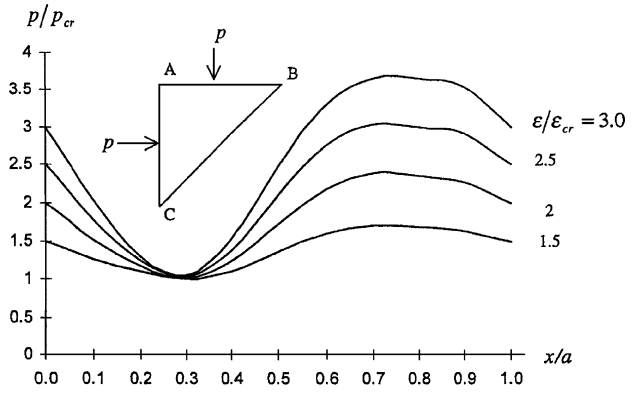

Fig. 6 Membrane stress distribution along perpendicular edges of right-angled isosceles triangular plate.

3. Membrane Stress Distribution and Postbuckling Path

Before buckling occurs in a perfectly flat triangular plate, the distribution of the edge compressive stresses is uniform. If the applied compressive stress increases beyond the critical stress, the distribution changes as soon as the plate buckles, due to the suppression of the differential plate shortening along its length.[18] The maximum edge stresses occur at the ends and decrease toward the middle of the edge of the plate.

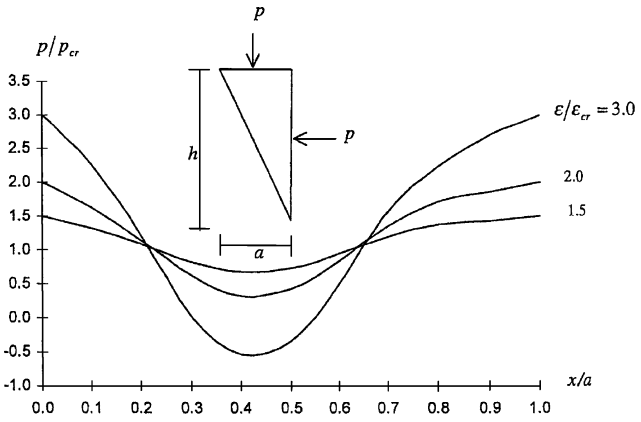

Fig. 7 Membrane stress distribution along perpendicular edge of right-angled isosceles triangular plate for $a/h=0.5$.

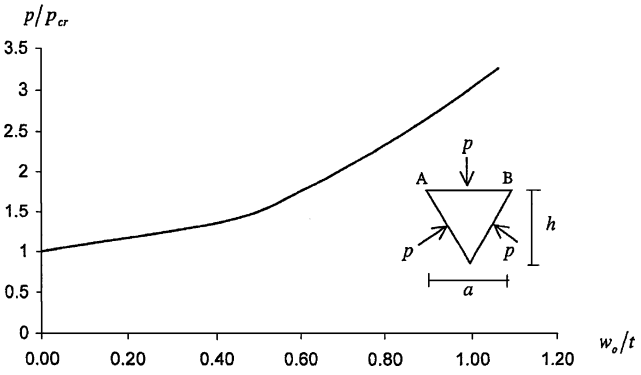

Fig. 8 Postbuckling path of an isosceles triangular simply supported plate under uniform compression with $a/h=1.0$.

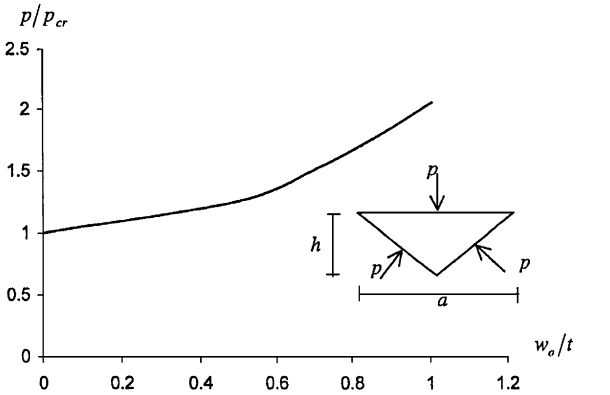

Fig. 9 Postbuckling path of an isosceles triangular simply supported plate under uniform compression with $a/h=2.0$.

The nonlinear procedure was used to calculate the membrane stress distribution of triangular plates with different geometries and loading, for which the edges are held straight. Figures 4–7 show the nondimensional postbuckled stress distribution for different width-to-height ratios at strains ε equal to various selected multiples of the elastic critical strain ε_{cr} and for different load cases. The figures show that with increasing applied strain, the stresses decrease substantially toward the middle of the edges, whereas with decreasing applied strain, the postbuckled stress distribution does not show such considerable variation.

The postbuckling paths of triangular plates with different geometries are shown in Figs. 8–10, where the deformation w_0 is that evaluated at $(x, y)=(a/2, b/2)$. The curves for all triangular plates exhibit the same characteristics; that is, there is a clear bifurcation between the primary path in which the triangular plate remains flat

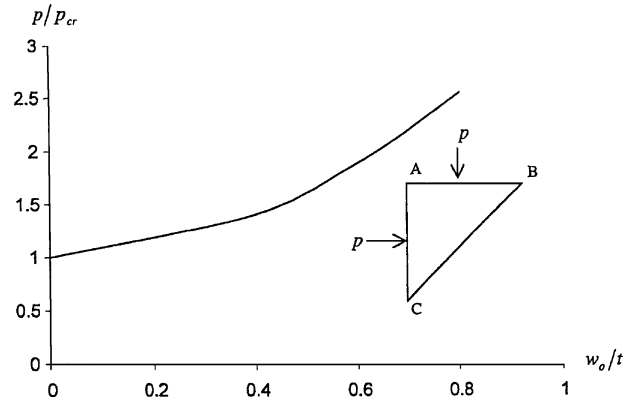

Fig. 10 Postbuckling path of a right-angled isosceles triangular simply supported plate.

and the secondary path that follows buckling into a nonflat configuration, and there is considerable stiffening in the advanced stages of postbuckling.

IV. Conclusions

A nonlinear method based on the principle of virtual work has been developed in this paper as a numerical procedure for the elastic postbuckling analysis of general simply supported plates. The procedure can be used for supports other than simple, but the polynomial shape functions need to be chosen accordingly. Area coordinates have been employed to express the geometry of the plates in simple form. The method is very efficient computationally.

The elastic postbuckling behavior of triangular plates with different geometries and loadings has been investigated. The stress distribution along the edges of triangular plates in the post–locally buckled domain has been determined for different geometrical parameters. These edge stresses show considerable variation and can even become tensile. Postbuckling paths for triangular plates with different geometries were illustrated graphically, and should be of use in configuring plate proportions in design.

Finally, the framework of the numerical scheme lends itself to implementation for investigating the postbuckling of triangular composite laminates and other advanced materials for which the use of the benign stiff postlocal buckling response is needed for efficient design.

Appendix A: Strain Matrices

$$[T_u] = \begin{pmatrix} \langle N^{(u)} \rangle_{,x} \\ \langle 0 \rangle \\ \langle N^{(u)} \rangle_{,y} \end{pmatrix}_{3 \times N_u}, \qquad [T_v] = \begin{pmatrix} \langle 0 \rangle \\ \langle N^{(v)} \rangle_{,y} \\ \langle N^{(v)} \rangle_{,x} \end{pmatrix}_{3 \times N_v}$$

$$\{\varepsilon_H\} = \begin{Bmatrix} \varepsilon_{x0} \\ \varepsilon_{y0} \\ \gamma_{xy0} \end{Bmatrix}, \qquad [T_w] = \begin{pmatrix} w_{,x} \langle N^{(w)} \rangle_{,x} \\ w_{,y} \langle N^{(w)} \rangle_{,y} \\ w_{,x} \langle N^{(w)} \rangle_{,y} + w_{,y} \langle N^{(w)} \rangle_{,x} \end{pmatrix}_{3 \times N_w}$$

$$[B_f] = \begin{pmatrix} -\langle N^{(w)} \rangle_{,xx} \\ -\langle N^{(w)} \rangle_{,yy} \\ -2\langle N^{(w)} \rangle_{,xy} \end{pmatrix}_{3 \times N_w}$$

Appendix B: Components of Nonlinear Stiffness Matrices and Forces

$$[T_{uu}]_{N_u \times N_u} = \int_{\mathcal{P}} [T_u]^T [D_m][T_u] \, d\mathcal{P}$$

$$[T_{uv}]_{N_u \times N_v} = \int_{\mathcal{P}} [T_u]^T [D_m][T_v] \, d\mathcal{P}$$

$$[T_{uw}]_{N_u \times N_w} = \int_{\mathcal{P}} [T_u]^T [D_m][T_w] \, d\mathcal{P}$$

$$[T_{vu}]_{N_{vu} \times N_u} = \int_{\mathcal{P}} [T_v]^T [D_m][T_u] \, d\mathcal{P}$$

$$[T_{vv}]_{N_v \times N_v} = \int_{\mathcal{P}} [T_v]^T [D_m][T_v] \, d\mathcal{P}$$

$$[T_{uw}]_{N_v \times N_w} = \int_{\mathcal{P}} [T_v]^T [D_m][T_w] \, d\mathcal{P}$$

$$[T_{wu}] = 2[T_{uw}]^T, \qquad [T_{wv}] = 2[T_{vw}]^T$$

$$\{F_u\} = \int_{\mathcal{P}} [T_u]^T [D_m]\{\varepsilon_H\} \, d\mathcal{P}, \qquad \{F_v\} = \int_{\mathcal{P}} [T_v]^T [D_m]\{\varepsilon_H\} \, d\mathcal{P}$$

$$\{F_w\} = \int_{\mathcal{P}} [T_w]^T [D_m]\{\varepsilon_H\} \, d\mathcal{P}$$

Appendix C: Components of Nonlinear Tangent Stiffness Matrices and Forces

$$[K_{\mathrm{NL}}]_{,j} = \frac{\partial}{\partial \hat{w}_j} [K_{\mathrm{NL}}] = \begin{pmatrix} [0]_{N_u \times N_u} & [0]_{N_u \times N_v} & [T_{uw}]_{,j} \\ [0]_{N_v \times N_u} & [0]_{N_v \times N_v} & [T_{vw}]_{,j} \\ [T_{wu}]_{,j} & [T_{wv}]_{,j} & [T_{ww}]_{,j} \end{pmatrix}$$

$$\{F\}_{,j} = \frac{\partial}{\partial \hat{w}_j} \{F\} = \begin{pmatrix} \{0\}_{N_u \times 1} \\ \{0\}_{N_v \times 1} \\ \{F_w\}_{,j} \end{pmatrix}$$

$$[T_{uw}]_{,j} = \frac{1}{2} \int_{\mathcal{P}} [T_u]^T [D_m][T_w]_{,j} \, d\mathcal{P} = \frac{1}{2} [T_{wu}]_{,j}$$

$$[T_{vw}]_{,j} = \frac{1}{2} \int_{\mathcal{P}} [T_v]^T [D_m][T_w]_{,j} \, d\mathcal{P} = \frac{1}{2} [T_{wv}]_{,j}$$

$$[T_{wu}]_{,j} = \frac{1}{2} \int_{\mathcal{P}} [T_w]^T [D_m][T_u]_{,j} \, d\mathcal{P}$$

$$[T_{wv}]_{,j} = \frac{1}{2} \int_{\mathcal{P}} [T_w]^T [D_m][T_v]_{,j} \, d\mathcal{P}$$

$$[T_{ww}]_{,j} = \frac{1}{2} \int_{\mathcal{P}} \left([T_w]_j^T [D_m][T_w] + [T_w]^T [D_m][T_w]_{,j} \right) d\mathcal{P}$$

$$\{F_w\}_j = \int_{\mathcal{P}} [T_w]_{,j}^T [D_m]\{\varepsilon_H\} \, d\mathcal{P}$$

where

$$[T_w]_{,j} = \frac{\partial}{\partial \hat{w}_j} [T_w] = \begin{pmatrix} N_{j,x}^{(w)} \langle N^{(w)} \rangle_{,x} \\ N_{j,y}^{(w)} \langle N^{(w)} \rangle_{,y} \\ N_{j,x}^{(w)} \langle N^{(w)} \rangle_{,y} + N_{j,y}^{(w)} \langle N^{(w)} \rangle_{,x} \end{pmatrix}_{3 \times N_w}$$

References

[1]Woinowsky-Krieger, S., "Berechnug der Ringsum Frei Aufliegenden Gleischeitigen Dreiecksplate," *Ing. Archive*, Vol. 4, 1933, pp. 254–262.

[2]Taylor, J. L., "Buckling and Vibration of Triangular Flat Plates," *Journal of the Royal Aeronautical Society*, Vol. 71, No. 682, 1967, pp. 727, 728.

[3]Klitchieff, J. M., "Buckling of Triangular Plates by Shearing Forces," *Quarterly Journal of Mechanics and Applied Mechanics*, Vol. 4, No. 3, 1951, pp. 257–259.

[4]Wittrick, W. H., "Symmetrical Buckling of Right-Angled Isosceles Triangular Plates," *Aeronautical Quarterly*, Vol. 5, No. 2, 1953, pp. 131–143.

[5]Pan, L. C., "Equilibrium Buckling and Vibration of 30–60–30 deg Triangular Plate Simply Supported at the Edges," *Acta Physica Sin.*, Vol. 3, 1956, pp. 212–245.

[6]Valisetty, R. R., and Reddy, A. D., "Design Data and Buckling of Laminated Composite Triangular Plates," Society of Automotive Engineers, SAE TP Series, SP-623, Warrendale, PA, 1985, pp. 25–29.

[7]Liew, K. M., and Wang, C. M., "Elastic Buckling of Rectangular Plates with Internal Curved Supports," *Journal of Structural Engineering*, Vol. 118, No. 6, 1992, pp. 1480–1493.

[8]Wang, C. M., and Liew, K. M., "Buckling of Triangular Plates under Uniform Compression," *Engineering Structures*, Vol. 16, No. 1, 1994, pp. 43–50.

[9]Jaunky, N., Knight, N. F., and Ambur, D., "Buckling Analysis of General Triangular Anisotropic Plates Using Polynomials," *AIAA Journal*, Vol. 33, No. 5, 1995, pp. 2414–2417.

[10]Azhari, M., and Bradford, M. A., "The Use of Bubble Functions for the Post-Local Buckling of Plate Assemblies by the Finite Strip Method," *International Journal for Numerical Methods in Engineering*, Vol. 38, No. 6, 1995, pp. 955–968.

[11]Jayachandran, S. A., and Vaidyanathan, C. V., "Post Critical Behaviour of Biaxially Compressed Plates on Elastic Foundations," *Computers and Structures*, Vol. 54, No. 2, 1995, pp. 239–246.

[12]Shen, H. S., and Lin, Z. Q., "Thermal Post-Buckling Analysis of Imperfect Laminated Plates," *Computers and Structures*, Vol. 57, No. 3, 1995, pp. 533–540.

[13]Hoon, K. H., and Khong, P. W., "The Semi-Energy and the Lower Bound Methods to the Post-Buckling of Plates," *Computers and Structures*, Vol. 58, No. 1, 1996, pp. 107–113.

[14]Shen, H. S., "Thermomechanical Post-Buckling Analysis of Imperfect Laminated Plates Using a Higher-Order Shear-Deformation Theory," *Computers and Structures*, Vol. 66, No. 4, 1998, pp. 395–409.

[15]Shen, H. S., "Thermal Postbuckling of Imperfect Laminated Shear-Deformation Plates on Two-Parameter Elastic Foundation," *Mechanics of Composite Materials and Structures*, Vol. 6, No. 3, 1999, pp. 207–228.

[16]Shen, H. S., "Thermal Postbuckling of Preloaded Shear-Deformable Laminated Plates," *Journal of Engineering Mechanics*, Vol. 126, No. 5, 2000, pp. 488–495.

[17]Bradford, M. A., and Hancock, G. J., "Elastic Interaction of Local and Lateral Buckling in Beams," *Thin-Walled Structures*, Vol. 2, No. 1, 1984, pp. 1–25.

[18]Allen, H. G., and Bulson, P. S., *Background to Buckling*, McGraw–Hill, London, 1980.

E. Johnson
Associate Editor